

Explainable Artificial Intelligence in Retinal Imaging for the detection of Systemic Diseases

Ayushi Raj Bhatt

Rajkumar Vaghashiya

Meghna Kulkarni

Dr Prakash Kamaraj

Abstract

Explainable Artificial Intelligence (AI) in the form of an interpretable and semiautomatic approach to stage grading ocular pathologies such as Diabetic retinopathy, Hypertensive retinopathy, and other retinopathies on the backdrop of major systemic diseases. The experimental study aims to evaluate an explainable staged grading process without using deep Convolutional Neural Networks (CNNs) directly. Many current CNN-based deep neural networks used for diagnosing retinal disorders might have appreciable performance but fail to pinpoint the basis driving their decisions. To improve these decisions' transparency, we have proposed a clinician-in-the-loop assisted intelligent workflow that performs a retinal vascular assessment on the fundus images to derive quantifiable and descriptive parameters. The retinal vessel parameters meta-data serve as hyper-parameters for better interpretation and explainability of decisions. The semiautomatic methodology aims to have a federated approach to AI in healthcare applications with more inputs and interpretations from clinicians. The baseline process involved in the machine learning pipeline through image processing techniques for optic disc detection, vessel segmentation, and arteriole/venule identifica-

1. Introduction

Retinal health is essential in monitoring of individual health since it is a direct extension of the vasculature of the central nervous system. Changes in the retinal vasculature, such as thickening/widening of venules and narrowing of arteries, as well as tortuosity of the vessels and branching pattern of the daughter vessels, have proven to be significant biomarkers for the detection of pathologies that serve as a backdrop to systemic disorders [31, 33, 36, 28].

1.1. Impact of Deep Learning (DL) based models

The most common pathology observed in retinal imaging is Diabetic retinopathy (DR), being one of the main

causes of blindness at the global level, especially in the working-age population [7]. Experiencing severe grades of DR in the working age group can cause severe loss in productivity. Deep Learning has become a key tool in terms of AI-assisted diagnosis of DR [5, 18]. There are also instances of Deep learning modules, such as CNNs that play a role in the classification of hypertensive retinopathy (HTR) [43]. Features such as the narrowing of vessels in the retina, vascular bleeding, and cotton wool spots play a role in the detection of retinopathy diseases of varied etiology. Deep learning has also helped improve the staging of diabetic retinopathy conditions [40].

1.2. Automated retinal AI for detection of diseases

The diagnosis of the majority of retinopathies from the fundus images by clinicians is based on visual clues such as abnormal retinal vasculature morphology, bleeding, exudates, hemorrhages, and so on. Thus, computer vision greatly underpins the automatic detection of retinal conditions via image processing techniques such as blood vessel segmentation, classification [4], optic disc detection, and exudate localization. When combined, these intelligent algorithms can help detect ocular-cum-systemic conditions such as hypertension, diabetic retinopathy, and atherosclerosis. There have been extensive CNN-based researches such as on the automatic grading of retinal vessels [30] and detection of lesions, microaneurysms, cotton wool spots, exudates, and retinal hemorrhages [3, 16, 21]. These techniques have attained appreciable performance comparable to that of trained ophthalmologists. Further, various systems have been developed for specific disease detection and management, such as for hypertensive retinopathy [1, 24].

1.3. The explainable AI

Explainable AI (XAI) are a modern-day example of having more accountable artificial intelligence systems where the results are open to interpretation, paving for better understanding by humans. XAI has been a conscious exploration in the realm of retinal imaging analysis as well [25]. However, there is always uncertainty when it comes to deep learning-based models of retinal diseases [39]. There is a

constant need for an analysis system better understood by an ophthalmologist to avoid erroneous diagnoses. The difficulty is also experienced in advanced imaging systems such as retinal OCT diagnosis [6]. There is a need to explore more on the domain with attributable risk factors with more qualitative and quantitative analysis [38].

1.4. Diseases in focus

Analysis of retinal vasculature could be extrapolated not just in ophthalmic conditions but in systemic diseases as well. The major systemic diseases that draw inference from the retinal vascular analysis are retinopathy, associated with the following conditions.

- Diabetes [13]
- Diabetic Nephropathy [20]
- Chronic kidney disease [45]
- Hypertension [9]
- Cardiovascular diseases [14]
- Neurocognitive diseases [10]
- Infectious diseases due to immunodeficiency [41, 42]
- Inflammatory diseases [17]

1.5. Retinal vascular parameters and retinopathies

Many of the above-mentioned research utilize black-box models, i.e., the specific decisions taken by the model to conclude are not explainable. Thus, such systems resist adoption by clinicians despite their great performance.

Apart from image processing techniques and deep learning methods, there is a need to explore more meaningful parameters that contribute to specific conditions. There have been significant findings that relate changes in the retinal vasculature to certain systemic diseases and retinopathies. Specific findings were noticed towards prediabetic and hypertensive conditions [31]. Measurement of arterio-venous ratio has been especially useful in the detection of hypertensive conditions [33, 36]. Alterations in the retinal vascular caliber (RVC) are observed during routine retina examination during pre-pathological and pathological states [20]. RVC has also indicated relevance in systemic disease conditions such as diabetic nephropathy and diabetic neuropathy.

Retinal vasculature parameters such as vascular tortuosity also have an impact on cardiovascular diseases. Retinal vascular tortuosity is associated with higher levels of blood pressure and HDL levels [12]. Retinal image-specific signs such as arterio-venous nicking have linear correlations with cardiovascular disorders, and hypertension [37]. Automated methods have been developed to quantify such parameters from color fundus images [32, 44].

Fractal dimension (FD) is an indicative parameter that analyzes retinal vasculature as a fractal; the geometric parameterization helps to analyze the branching pattern of retinal vessels [28]. Fractal dimension has been associated

with significance in conditions like stroke [11, 27]. The vascular parameters-based approach would serve as an effective modus operandi for explainable AI in healthcare.

2. Method

2.1. Diseases and corresponding datasets used in the study

This study is focused on the detection and stage-grading of three retinopathies, namely, Diabetic Retinopathy (DR), Hypertensive Retinopathy (HTR) and Diabetic Macular Edema (ME). Quite a few retinal datasets are available for research purpose and additional analysis. Publicly available datasets are especially important to analyze further, given the additional confounding factors of varying datasets by ethnicity, age, sex, and other etiological factors. Modern imaging analysis methods through powerful computation methods such as machine learning help in drawing additional inferences [23].

The dataset used in the study for DR and Macular Edema:

IDRID [35]

The datasets used in the study for HTR:

IDRID [35]

AVRDB [2]

JSIEC Images (Severe Hypertensive retinopathy category) [22]

3. Fundus Image Gradability Analysis

3.1. Grability analysis criteria

Fundus photographs acquired from the respective datasets were filtered based on the criteria of the visibility of four major arterioles and venules. The images were additionally analyzed to rule out the ones with prevailing co-morbidities.

3.2. Diabetic Retinopathy Dataset Analysis

A total of 516 images filtered out from the IDRID dataset were considered for DR analysis. The data analysis and filtering process for DR dataset is shown in Fig. 1.

The grade wise interpretation for multi-class classification is based on the disease severity levels as specified:

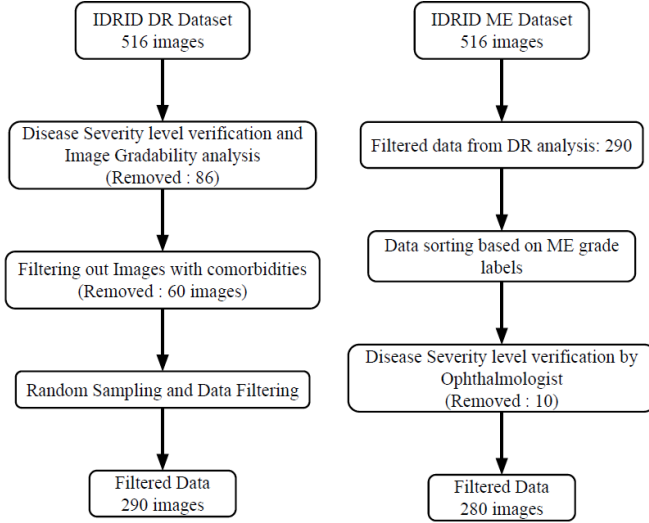


Figure 1: Filtering workflow for DR and ME datasets

Severity Grade	Train Data	Test Data
Grade 0	52	33
Grade 1	20	5
Grade 2	51	32
Grade 3	40	19
Grade 4	32	6

Table 1: Sample division in Diabetic Retinopathy Dataset

- Grade 0: Absence of DR
- Grade 1: Mild DR
- Grade 2: Moderate DR
- Grade 3: Severe DR
- Grade 4: Signs of proliferative DR

The final data sample distribution for DR is specified in Table 1. The binary grade classification was considered on the presence or absence of the disease i.e. the Grade 0 signifies the absence and the remaining higher grades signify the presence of the disease.

3.3. Diabetic Macular Edema Dataset Analysis

516 images from the IDRID dataset for Diabetic Macular Edema (ME) were filtered out and randomly sampled for the image analysis. The data analysis and filtering process for ME dataset is shown in Fig. 1, and the final data sample distribution for ME is specified in Table 2. The grade wise interpretation is based on the disease severity levels as follows:

- Grade 0: No visible exudates
- Grade 1: Shortest distance between macula and exudates $>$ one optic disc diameter

Grade 2: Shortest distance between macula and exudates \leq one optic disc diameter

Severity Grade	Train Data	Test Data
Grade 0	82	41
Grade 1	14	9
Grade 2	94	40

Table 2: Sample division in Macular Edema Dataset

3.4. Hypertensive Retinopathy Dataset Analysis

A total of 66 hypertensive retinopathy images, combined from the AVRDB and the JSIEC dataset, were used for the analysis of higher grades of HTR. The control images (Grade 0) were taken from the IDRID dataset after ensuring the absence of comorbidities. The data collection, filtering and selection procedure is specified as follows is specified in Fig. 2. The final data sample distribution for HTR is specified in Table 2.

Due to the lack of test data, 80-20 ratio split on the filtered data was used for training and testing the model respectively. The grade wise interpretation is based on the following disease severity levels:

- Grade 0: No visible abnormalities
- Grade 1: Diffuse arteriolar narrowing
- Grade 2: Grade 1 with focal arteriolar constriction
- Grade 3: Grade 2 with retinal hemorrhage
- Grade 4: Grade 3 with hard exudates, retinal edema, and optic disc swelling

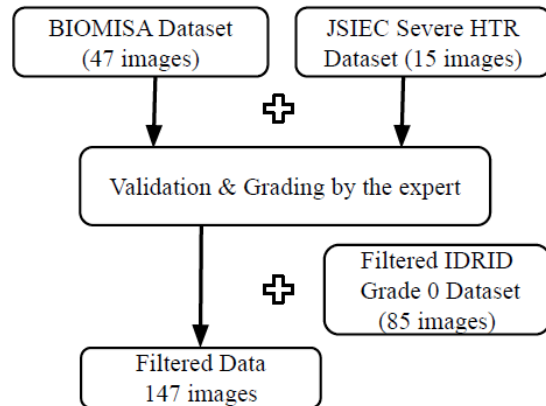


Figure 2: Filtering workflow for HTR dataset

Severity Grade	Train Data
Grade 0	85
Grade 1	11
Grade 2	15
Grade 3	20
Grade 4	16

Table 3: Sample division in Hypertensive Retinopathy Dataset

4. Calculation of Retinal Vascular Parameters

The filtered data was graded and retinal vessel characteristics were extracted using the Singapore ‘T’ Vessel Assessment (SIVA) software [26]. The semi-automated retinal vascular network evaluation was based on the analysis of vessels from the center of the optic disc and then to three successive zones corresponding to 0.5 (zone A), 1 (zone B) and 2 (zone C) optic disc diameters, as shown in Fig. 3. The parameters analyzed, per vessels, arterioles, and venules, were as follows:

- Central retinal arteriole equivalent (CRAE)
- Central retinal venule equivalent (CRVE)
- Arteriovenous ratio (AVR)
- Fractal dimension (FD)
- Mean vessel width (MW)
- Standard deviation of vessel width (STDW)
- Tortuosity (TORT)
- Length to diameter ratio (LDR)
- Branching coefficient (BC)
- Asymmetry Factor (AF)
- Branching angle (BA)
- Asymmetry angle (AA)
- Junction exponent (JE)
- Number of branches & number of first branches
- Number of arterioles and venules

An *a* beside the parameter, for *e.g.* FD_a , denotes arteriolar measurement while a *v*, for *e.g.* FD_v denotes venular measurement. The derivation for the mentioned parameters is specified in [26]. The workflow for the parametric calculations is specified in Fig. 4.

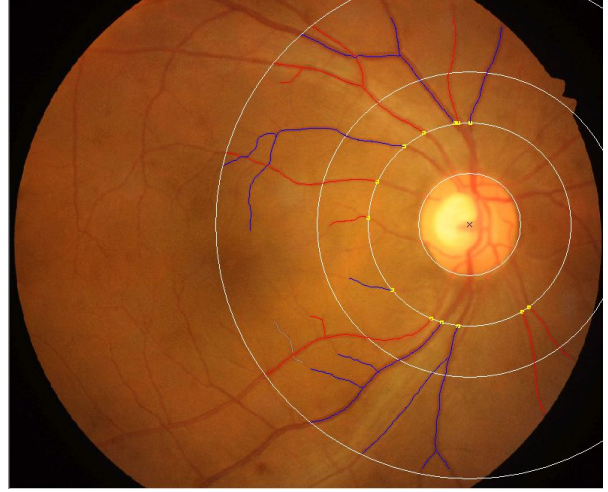


Figure 3: Vessel classification with retinal zones in SIVA

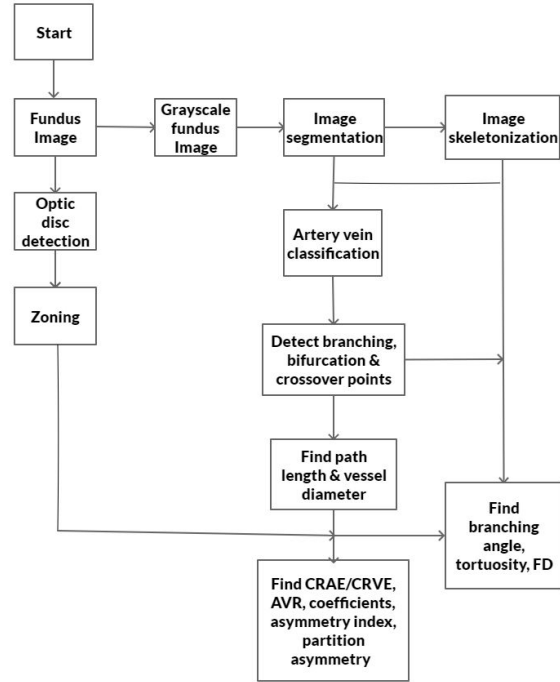


Figure 4: SIVA-based parametric quantification workflow

4.1. Stepwise Linear Regression Analysis

A stepwise multi-linear regression analysis was performed using IBM SPSS v23 to analyze the study parameters and to check for multicollinearity in the input retinal parameters.

4.1.1 DR data analysis

The input variables statistically significantly predicted the DR severity stage, $F(51, 238) = 3.118, p < .0005, R^2 =$

.401. No variables were found that added statistically significantly to the prediction, $p < .05$. As per the analysis, the parameters Baa, AD2a, BAv, AAv, Bat, and AD2t were excluded from the study. The details of the tests are provided in the supplementary.

4.1.2 HTR data analysis

The input variables statistically significantly predicted the HTR severity stage, $F(51, 95) = 6.850$, $p < .0005$, $R^2 = .786$. The variables AVR (of both zone B and C), arteriolar MW and BMW, and arteriolar NumLDR added statistically significantly to the prediction, $p < .05$. As per the analysis, the parameters BAa, AD2a, BAv, AAv, BAAt, and AAt were excluded from the study. The details of the tests are provided in the supplementary.

4.1.3 ME Data Analysis

The input variables statistically significantly predicted the ME severity stage, $F(51, 228) = 1.567$, $p < .0005$, $R^2 = .260$. The variables CRVE (of both zone B and C) added statistically significantly to the prediction, $p < .05$. As per the analysis, the parameters BAa, AD2a, BAv, AAv, AD1t, and AD2t were excluded from the study. The details of the tests are provided in the supplementary.

Most of the retinal parameters under consideration in this study convey certain unique and causal information about the retinal vasculature morphology in relation to the disease being diagnosed. There is a possibility of spurious correlation among the input parameters that might negatively interfere and affect the multi-linear regression analysis.

5. Machine Learning Study Design

The experiment was conducted on a cloud-based compute platform, Google Colab [15]. Standard machine learning algorithms for classification were evaluated on the data set, mostly using scikit-learn [34], namely:

- K-Neighbors Classifier (KNC)
- Extreme Gradient Boosting (XGB) [8]
- Random Forest Classifier (RFC)
- Multi-Layer Perceptron Classifier (MLP)
- Decision Tree Classifier (DTC)
- Gaussian Naive Bayes Classifier (GNB)
- Gaussian Process Classifier (GPC)
- AdaBoost Classifier (ABC)
- Quadratic Discriminant Analysis (QDA)
- Logistic Regression (LR)
- Support Vector Classifier (SVC)

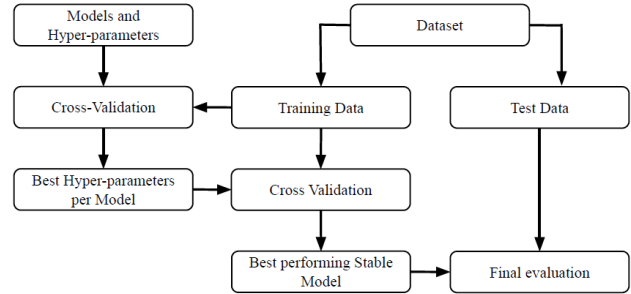


Figure 5: ML model evaluation workflow

For feature scaling, the data of each continuous parameter is transformed using Min-Max scaling technique to normalize the variance to a standard range i.e. between 0 and 1. This is done to balance the effect of parameters, e.g. CRVE and CRAE, typically having higher values compared to the rest, e.g. AVR and FD. Following this, tSNE was utilized to view the class representations and check for inter-class separability.

Cross-validation has been utilized to ensure consistent performance with minimal tolerance in the accuracy. Nested cross-validation on the training dataset was carried out using 4 inner folds for determination of the optimal model hyperparameters, and 6 outer folds for determination of the model performance and stability on the dataset. The top 4 performing models were then evaluated on the test set to determine the final model performance. The workflow of model hyperparameter selection and evaluation is summarized in Fig. 5.

A weighted one-vs-rest Receiver Operating Characteristics-Area Under the Curve (ROC-AUC) [19] the scheme was used as the scoring criteria. ROCAUC is a parameter-agnostic graphical performance metric for binary classification problems used to depict how well a discriminator model minimizes the overlap between the two class distributions, the diseased and the non-diseased. ROC is the probability curve derived from the evaluation of the test samples while AUC denotes the area under that curve. $AUC \leq 0.5$ implies model performs no better than a random guess, while $AUC > 0.5$ implies the model is able to discriminate well between the classes, with AUC of 1 being the maximum possible score. It is adapted for multi-class problems by pitting one class against the rest (one-vs-rest).

Range of Hyper-parameters

- KNC: weights : [uniform, distance]
- algorithm: [auto, ball tree, kd tree]
- XGB: learning_rate: [10^{-3} , 10^{-2} , 10^{-1}]
- n_estimators: [100, 120, 140]
- RFC: max_depth: [1, 2, 4, 8, 16, 32, 64, None]
- n_estimators: [8,9,10,11,12,13, 100, 120, 150, 200]
- min_samples_split: [1,2,3]

MLP: hidden_layer_sizes: [10, 20, 40, 60, 80, 100, 120, 150, 200]
 DTC: max_depth: [1, 2, 4, 8, 16, 32, None]
 min_samples_split: [1,2,3]
 criterion: [gini, entropy]
 GNB: var_smoothing: [1e-9]
 GPC: max_iter_predict: [25, 50, 75, 100, 120, 150]
 ABC: n_estimators: [10, 20, 40, 50, 70, 100, 120]
 QDA: tol: [1e-4]
 LR : max_iter: [50, 100, 500, 100, 5000, 10000]
 C: [10⁻⁴, 10⁻³, 10⁻², 10¹, 10⁰, 10¹, 10²]
 SVC: C: [10⁻⁴, 10⁻³, 10⁻², 10¹, 10⁰, 10¹, 10²]
 kernel: [poly, rbf, sigmoid]

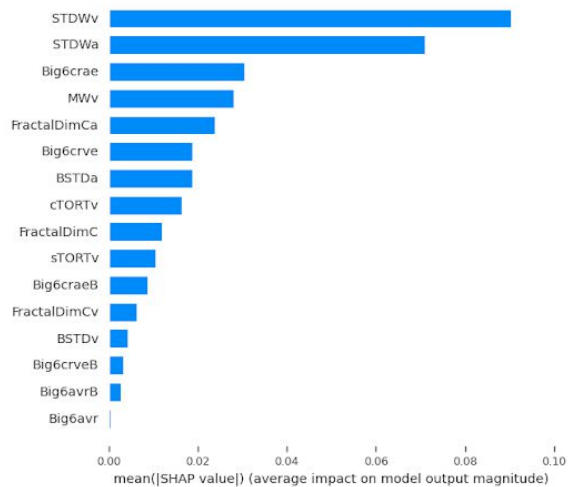
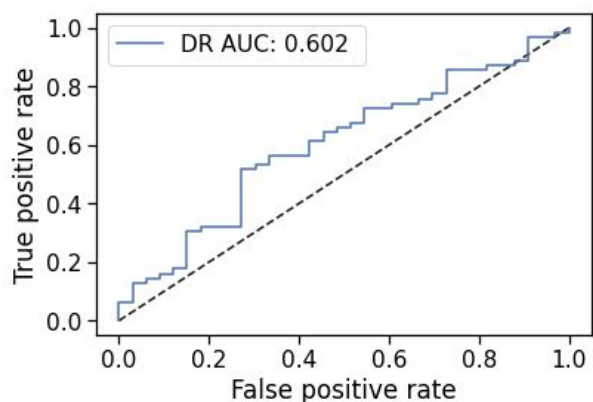


Figure 6: (a) DR Detection Results (b) DR Detection Feature Importance

6. Classification Results

6.1. DR Detection Results

ROC-AUC of 0.602 has been achieved for DR detection as depicted in Fig. 6. The best model is XGB with hyper-

parameters learning_rate: 0.01 and n_estimators: 140.

For the explanation of the results, a game-theoretic approach named SHAP [29] is used to analyze the individual impact of the input retinal features in the decision-making process. The feature analysis for DR detection reveals that the vessel width deviations (STDW_a and STDW_v) and the central venular equivalent (CRVE) are the leading parameters driving the decision on the detection of the disease.

6.2. DR Stage Grading Results

For DR stage grading, the performance of ~0.67 has been attained for stages 1 and 2, while ROCAUC of 0.812 and 0.863 has been attained for the most severe stages i.e. Grade 3 and 4 respectively as depicted in Fig. 7. The best model is Random Forest Classifier (RFC) with hyperparameters max_depth: 8, min_samples split: 3, and n_estimators: 100.

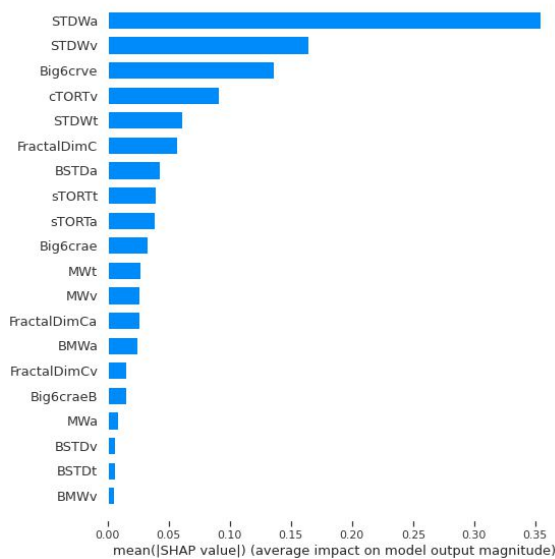
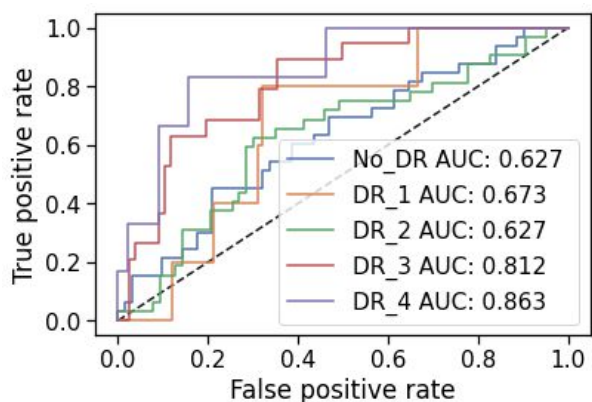


Figure 7: (a) DR Stage grading Results (b) DR Stage grading Feature Importance

Consistent with the DR detection, the SHAP feature analysis reveals that the vessel width deviations (STDW_a and STDW_v) and the central venular equivalent (CRVE) are the leading parameters driving the decision on the DR stage-grading as well.

6.3. HTR Detection Results

For HTR detection, high performance with ROCAUC of 0.937 has been achieved as depicted in Fig. 8. The best model is XGB with hyperparameters learning_rate: 0.01 and n_estimators: 120. The SHAP analysis reveals that the tortuosity (curvature tortuosity in this case) is the primary deciding factor in HTR detection, and this fact has been corroborated by past findings from retinal experts.

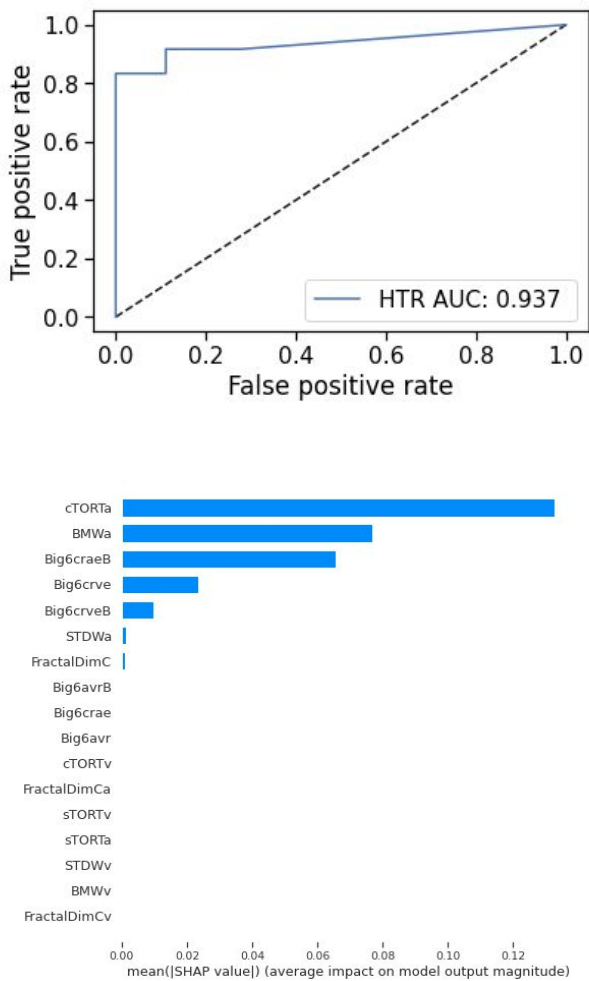


Figure 8: (a) HTR Detection Results (b) HTR Detection Feature Importance

6.4. HTR Stage Grading

For HTR stage grading, a high-performance ROC-AUC ~ 0.95 has been obtained for stages 0,2 and 3, while stage

1 has ROCAUC 0.877 and stage 4 has ROCAUC 0.721 respectively, as depicted in Fig. 9. The best model is Random Forest Classifier (RFC) with hyperparameters max_depth: 2, min_samples_split: 2, and n_estimators: 100. The SHAP feature analysis reveals that the central venular and arteriolar equivalents as well as parameters like fractal dimension jointly contribute towards the stage-grading of the disease.

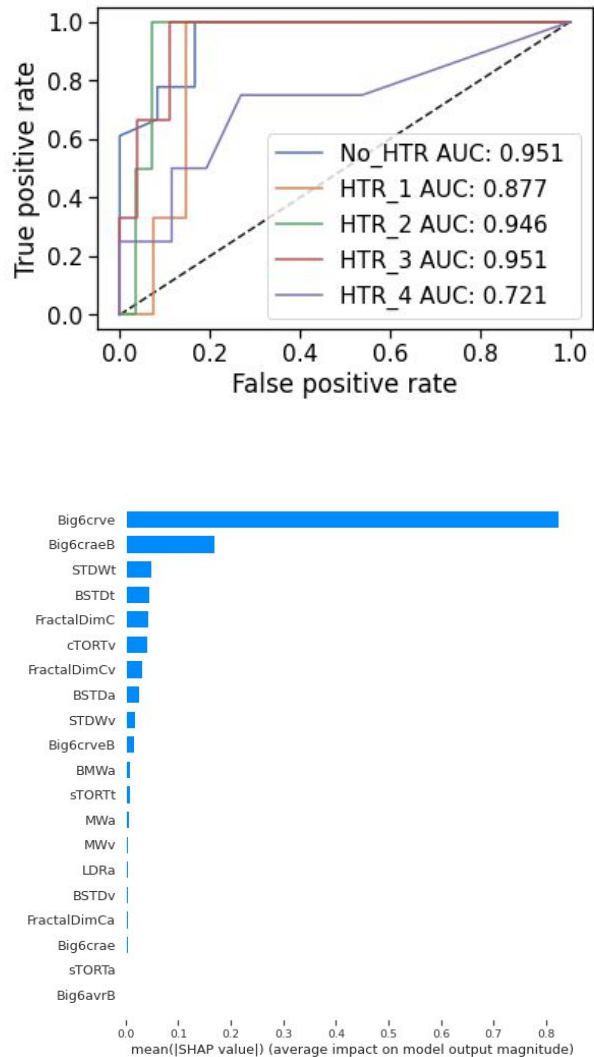
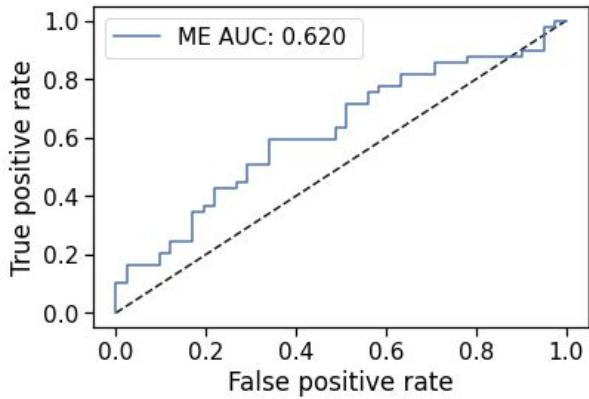


Figure 9: (a) HTR Stage grading Results (b) HTR Stage grading Feature Importance

6.5. ME Detection Results

The performance in ME is similar to that achieved in DR detection. For ME detection, ROC-AUC of 0.602 has been achieved for DR detection as depicted in Fig. 10. The best model is XGB with hyperparameters learning_rate: 0.001 and n_estimators: 140. The SHAP analysis reveals that the detection depends on a lot of factors such as central vessel

equivalents(Zone B CRAE and CRVE), arteriolar vessel tortuosity (cTORT), and mean arteriolar width (Zone B MWa).



making process as well result interpretation of the intelligent models.

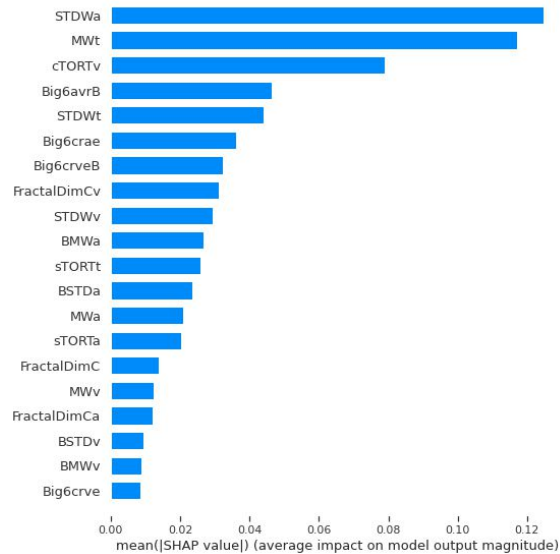
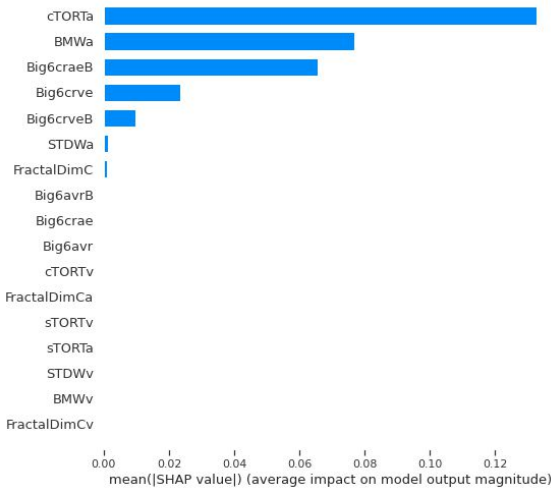
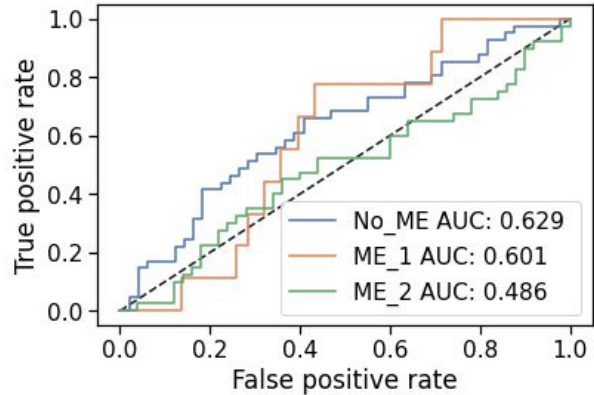


Figure 10: (a) ME Detection Results (b) ME Detection Feature Importance

Figure 11: (a) ME Stage grading Results (b) ME Stage grading Feature Importance

6.6. ME Stage Grading

For ME stage-grading, the performance of ROC-AUC ~ 0.61 for Grades 0 and 1, while a ROC-AUC of 0.468 for Grade 2 is achieved as depicted in Fig. 11. The best model is AdaBoost Classifier (ABC) with hyperparameters $n_estimators: 40$.

Similar to the ME detection, the SHAP feature analysis reveals that the ME stage grading jointly depends on factors such as central vessel equivalents (CRAE and CRVE), vessel tortuosity (cTORT), and fractal dimension (Zone C venular FD) as observed above. The final results of the study are shown in Table 4. This the study explores how the changes in vascular morphology, when quantified and employed, could serve as the much-needed explanatory biomarkers that help in the understanding of the decision-

Task	Best Model	Train Perf. ROCAUC	Test Perf. ROCAUC	Train Time in min
Disease Detection				
DR	XGB	.776 \pm .095	.602	8.077
HTR	XGB	.986 \pm .027	.937	.048
ME	XGB	.650 \pm .115	.620	0.986
Disease Grading				
DR	RFC	.799 \pm .049	.721	2.675
HTR	RFC	.976 \pm .009	.889	1.877
ME	ABC	.486 \pm .077	.572	2.735

Table 4: Experiment Results

7. Conclusion and Future work

Despite having a relatively smaller dataset to work with, a multivariate approach of specific retinal vascular parameters have shown a reasonable association with retinal signs caused due to systemic pathologies. Deep learning methods need a larger dataset to work, needing at least 2000 images to have reasonable classifier results. The retinal vascular parameters accounting for reliable parameters showing specific associations to systemic diseases, we could have better results on larger datasets with dedicated preprocessing and filtering for other comorbidities that could affect the co-variate results. Better literature review and clinical studies for the specific parameters in tandem with other secondary clinical parameters will lead to better results and thus paving the way for explainable AI of retinal vascular analysis.

References

- [1] S. Akbar, M. U. Akram, M. Sharif, A. Tariq, and S. A. Khan. Decision support system for detection of hypertensive retinopathy using arteriovenous ratio. *Artificial intelligence in medicine*, 90:15–24, 2018. Publisher: Elsevier. **1**
- [2] S. Akbar, T. Hassan, M. U. Akram, U. U. Yasin, and I. Basit. AVRDB: annotated dataset for vessel segmentation and calculation of arteriovenous ratio. pages 129–134. The Steering Committee of The World Congress in Computer Science, Computer . . . , 2017. **2**
- [3] M. U. Akram, S. Akbar, T. Hassan, S. G. Khawaja, U. Yasin, and I. Basit. Data on fundus images for vessels segmentation, detection of hypertensive retinopathy, diabetic retinopathy and papilledema. *Data in brief*, 29:105282, 2020. Publisher: Elsevier. **1**
- [4] M. Arsalan, M. Owais, T. Mahmood, S. W. Cho, and K. R. Park. Aiding the diagnosis of diabetic and hypertensive retinopathy using artificial intelligence-based semantic segmentation. *Journal of clinical medicine*, 8(9):1446, 2019. Publisher: MDPI. **1**
- [5] N. Asiri, M. Hussain, F. Al Adel, and N. Alzaidi. Deep learning based computer-aided diagnosis systems for diabetic retinopathy: A survey. *Artificial intelligence in medicine*, 99:101701, 2019. Publisher: Elsevier. **1**
- [6] A. S. Brar. Explainable AI for retinal OCT diagnosis. 2021. Publisher: University of Waterloo. **2**
- [7] R. Cheloni, S. A. Gandolfi, C. Signorelli, and A. Odone. Global prevalence of diabetic retinopathy: protocol for a systematic review and meta-analysis. *BMJ open*, 9(3):e022188, 2019. Publisher: British Medical Journal Publishing Group. **1**
- [8] T. Chen and C. Guestrin. Xgboost: A scalable tree boosting system. pages 785–794, 2016. **5**
- [9] C. Y.-I. Cheung, M. K. Ikram, C. Sabanayagam, and T. Y. Wong. Retinal microvasculature as a model to study the manifestations of hypertension. *Hypertension*, 60(5):1094–1103, 2012. Publisher: Am Heart Assoc. **2**
- [10] C. Y.-I. Cheung, S. Ong, M. K. Ikram, Y. T. Ong, C. P. Chen, N. Venketasubramanian, and T. Y. Wong. Retinal vascular fractal dimension is associated with cognitive dysfunction. *Journal of Stroke and Cerebrovascular Diseases*, 23(1):43–50, 2014. Publisher: Elsevier. **2**
- [11] C. Y.-I. Cheung, W. T. Tay, M. K. Ikram, Y. T. Ong, D. A. De Silva, K. Y. Chow, and T. Y. Wong. Retinal microvascular changes and risk of stroke: the Singapore Malay Eye Study. *Stroke*, 44(9):2402–2408, 2013. Publisher: Am Heart Assoc. **2**
- [12] C. Y.-I. Cheung, Y. Zheng, W. Hsu, M. L. Lee, Q. P. Lau, P. Mitchell, J. J. Wang, R. Klein, and T. Y. Wong. Retinal vascular tortuosity, blood pressure, and cardiovascular risk factors. *Ophthalmology*, 118(5):812–818, 2011. Publisher: Elsevier. **2**
- [13] R. Crosby-Nwaobi, L. Z. Heng, and S. Sivaprasad. Retinal vascular calibre, geometry and progression of diabetic retinopathy in type 2 diabetes mellitus. *Ophthalmologica*, 228(2):84–92, 2012. Publisher: Karger Publishers. **2**
- [14] A. Deiseroth, T. Marcin, C. Berger, D. Infanger, J. Schäfer, B. Bannert, A. Schmidt-Trucksäss, R. E. Voll, D. Kyburz, and H. Hanssen. Retinal vessel diameters and physical activity in patients with mild to moderate rheumatic disease without cardiovascular comorbidities. *Frontiers in physiology*, 9:176, 2018. Publisher: Frontiers Media SA. **2**
- [15] B. Ekaba. Google colabatory. *Building Machine Learning and Deep Learning Models on Google Cloud Platform; A Comprehensive Guide for Beginners*, 2019. **5**
- [16] K. N. Fatima, M. U. Akram, and S. A. Bazaz. Papilledema detection in fundus images using hybrid feature set. pages 1–4. IEEE, 2015. **1**
- [17] A. J. Green, S. McQuaid, S. L. Hauser, I. V. Allen, and R. Lyness. Ocular pathology in multiple sclerosis: retinal atrophy and inflammation irrespective of disease duration. *Brain*, 133(6):1591–1601, 2010. Publisher: Oxford University Press. **2**
- [18] V. Gulshan, L. Peng, M. Coram, M. C. Stumpe, D. Wu, A. Narayanaswamy, S. Venugopalan, K. Widner, T. Madams, and J. Cuadros. Development and validation of a deep learning algorithm for detection of diabetic retinopathy in retinal fundus photographs. *Jama*, 316(22):2402–2410, 2016. Publisher: American Medical Association. **1**
- [19] K. Hajian-Tilaki. Receiver operating characteristic (ROC) curve analysis for medical diagnostic test evaluation. *Caspian journal of internal medicine*, 4(2):627, 2013. Publisher: Babol University of Medical Sciences. **5**
- [20] M. K. Ikram, C. Y. Cheung, M. Lorenzi, R. Klein, T. L. Jones, T. Y. Wong, and NIH/JDRF Workshop on Retinal Biomarker for Diabetes Group. Retinal vascular caliber as a biomarker for diabetes microvascular complications. *Diabetes care*, 36(3):750–759, 2013. Publisher: Am Diabetes Assoc. **2**
- [21] S. Irshad, M. Salman, M. U. Akram, and U. Yasin. Automated detection of cotton wool spots for the diagnosis of hypertensive retinopathy. pages 121–124. IEEE, 2014. **1**
- [22] Joint Shantou International Eye Centre (JSIEC). 1000 fundus images with 39 categories., 2019. **2**

- [23] S. M. Khan, X. Liu, S. Nath, E. Korot, L. Faes, S. K. Wagner, P. A. Keane, N. J. Sebire, M. J. Burton, and A. K. Denniston. A global review of publicly available datasets for ophthalmological imaging: barriers to access, usability, and generalisability. *The Lancet Digital Health*, 3(1):e51–e66, 2021. Publisher: Elsevier. [2](#)
- [24] S. Khitran, M. U. Akram, A. Usman, and U. Yasin. Automated system for the detection of hypertensive retinopathy. pages 1–6. IEEE, 2014. [1](#)
- [25] A. Kind and G. Azzopardi. An explainable AI-based computer aided detection system for diabetic retinopathy using retinal fundus images. pages 457–468. Springer, 2019. [1](#)
- [26] Q. P. Lau, M. L. Lee, W. Hsu, T. Y. Wong, E. Ng, U. Acharya, A. Campillo, and J. Suri. The singapore eye vessel assessment system. *Image analysis and modeling in ophthalmology*, pages 143–160, 2014. Publisher: CRC Press Boca Raton, FL. [4](#)
- [27] S. Lemmens, A. Devulder, K. Van Keer, J. Bierkens, P. De Boever, and I. Stalmans. Systematic review on fractal dimension of the retinal vasculature in neurodegeneration and stroke: assessment of a potential biomarker. *Frontiers in neuroscience*, 14:16, 2020. Publisher: Frontiers Media SA. [2](#)
- [28] G. Liew, J. J. Wang, N. Cheung, Y. P. Zhang, W. Hsu, M. L. Lee, P. Mitchell, G. Tikellis, B. Taylor, and T. Y. Wong. The retinal vasculature as a fractal: methodology, reliability, and relationship to blood pressure. *Ophthalmology*, 115(11):1951–1956, 2008. Publisher: Elsevier. [1](#), [2](#)
- [29] S. M. Lundberg and S.-I. Lee. A unified approach to interpreting model predictions. *Advances in neural information processing systems*, 30, 2017. [6](#)
- [30] D. Maji and A. A. Sekh. Automatic grading of retinal blood vessel in deep retinal image diagnosis. *Journal of Medical Systems*, 44(10):1–14, 2020. Publisher: Springer. [1](#)
- [31] T. T. Nguyen, J. J. Wang, and T. Y. Wong. Retinal vascular changes in pre-diabetes and prehypertension: new findings and their research and clinical implications. *Diabetes care*, 30(10):2708–2715, 2007. Publisher: Am Diabetes Assoc. [1](#), [2](#)
- [32] U. T. Nguyen, A. Bhuiyan, L. A. Park, R. Kawasaki, T. Y. Wong, J. J. Wang, P. Mitchell, and K. Ramamohanarao. An automated method for retinal arteriovenous nicking quantification from color fundus images. *IEEE Transactions on Biomedical Engineering*, 60(11):3194–3203, 2013. Publisher: IEEE. [2](#)
- [33] H. M. Pakter, E. Ferlin, S. C. Fuchs, M. K. Maestri, R. S. Moraes, G. Nunes, L. B. Moreira, M. Gus, and F. D. Fuchs. Measuring arteriolar-to-venous ratio in retinal photography of patients with hypertension: development and application of a new semi-automated method. *American journal of hypertension*, 18(3):417–421, 2005. Publisher: Oxford University Press. [1](#), [2](#)
- [34] F. Pedregosa, G. Varoquaux, A. Gramfort, V. Michel, B. Thirion, O. Grisel, M. Blondel, P. Prettenhofer, R. Weiss, and V. Dubourg. Scikit-learn: Machine learning in Python. *the Journal of machine Learning research*, 12:2825–2830, 2011. Publisher: JMLR. org. [5](#)
- [35] P. Prasanna, P. Samiksha, K. Ravi, K. Manesh, D. Girish, S. Vivek, and M. Fabrice. Indian diabetic retinopathy image dataset (idrid). *IEEE Dataport*, 2018. [2](#)
- [36] A. Rani and D. Mittal. Measurement of arterio-venous ratio for detection of hypertensive retinopathy through digital color fundus images. *Journal of Biomedical Engineering and Medical Imaging*, 2(5):35, 2015. [1](#), [2](#)
- [37] S. SHELburne, J. L. HAWLEY, and A. McGee. Retinal arteriovenous nicking: relation to enlargement of the heart in ambulatory patients with hypertension. *Archives of Internal Medicine*, 69(2):213–221, 1942. Publisher: American Medical Association. [2](#)
- [38] A. Singh, S. Sengupta, A. R. Mohammed, I. Faruq, V. Jayakumar, J. Zelek, and V. Lakshminarayanan. What is the optimal attribution method for explainable ophthalmic disease classification? pages 21–31. Springer, 2020. [2](#)
- [39] A. Singh, S. Sengupta, M. A. Rasheed, V. Jayakumar, and V. Lakshminarayanan. Uncertainty aware and explainable diagnosis of retinal disease. volume 11601, pages 116–125. SPIE, 2021. [1](#)
- [40] H. Takahashi, H. Tampo, Y. Arai, Y. Inoue, and H. Kawashima. Applying artificial intelligence to disease staging: Deep learning for improved staging of diabetic retinopathy. *PloS one*, 12(6):e0179790, 2017. Publisher: Public Library of Science San Francisco, CA USA. [1](#)
- [41] P. Tan, D. C. Lye, T. K. Yeo, C. Y. Cheung, T.-L. Thein, J. G. Wong, R. Agrawal, L.-J. Li, T.-Y. Wong, and V. C. Gan. A prospective case-control study to investigate retinal microvascular changes in acute dengue infection. *Scientific Reports*, 5(1):1–8, 2015. Publisher: Nature Publishing Group. [2](#)
- [42] P. B. Tan, O. K. Hee, C. Cheung, T. K. Yeo, R. Agrawal, J. Ng, T. H. Lim, T. Y. Wong, and S. C. Teoh. Retinal vascular parameter variations in patients with human immunodeficiency virus. *Investigative ophthalmology & visual science*, 54(13):7962–7967, 2013. Publisher: The Association for Research in Vision and Ophthalmology. [2](#)
- [43] B. K. Triwijoyo, W. Budiharto, and E. Abdurachman. The classification of hypertensive retinopathy using convolutional neural network. *Procedia Computer Science*, 116:166–173, 2017. Publisher: Elsevier. [1](#)
- [44] J. Wigdahl, P. Guimarães, G. Leontidis, A. Triantafyllou, and A. Ruggeri. Automatic Gunn and Salus sign quantification in retinal images. pages 5251–5254. IEEE, 2015. [2](#)
- [45] T. Y. Wong, D. Xu, D. Ting, S. Nusinovici, C. Cheung, T. E. Shyong, C.-Y. Cheng, M. L. Lee, W. Hsu, and C. Sabanayagam. Artificial intelligence deep learning system for predicting chronic kidney disease from retinal images. *Investigative Ophthalmology & Visual Science*, 60(9):1468–1468, 2019. Publisher: The Association for Research in Vision and Ophthalmology. [2](#)